

Table 2 Association between clinicopathologic characteristics and extracapsular invasion in patients with liver metastasis

Variable	ECI-positive (<i>n</i> = 47)	ECI-negative (<i>n</i> = 50)	<i>p</i>
Sex			0.1303
Male	21	30	
Female	26	20	
Age			0.2385
<65 years	30	26	
≥65 years	17	24	
Primary site			0.8137
Colon	33	34	
Rectum	14	16	
pT			0.6536
pT1–pT3	29	33	
pT4	18	17	
No. of positive LNs			0.0022
1–2	17	34	
>2	30	16	
Histology			0.9376
Well/mod. differentiated	44	47	
Poorly differentiated/ mucinous	3	3	
Lymphovascular invasion			0.0941
Negative	13	22	
Positive	34	28	
Timing of development			0.0238
Metachronous	6	16	
Synchronous	41	34	
No. of metastases			0.0001
1–3	21	41	
≥4	26	9	
Maximum diameter			0.5205
<4 cm	32	37	
≥4 cm	15	13	
Tumor distribution			0.2551
Unilateral	21	28	
Bilateral	26	22	

adenocarcinoma were referred to the Department of General Surgical Science, Graduate School of Medicine, Gunma University. Of these patients, the primary tumor was associated with regional LN metastases in 97 patients. Twenty-four patients had no regional lymph-node metastases from a colorectal tumor, and all of them received liver resection. The patients who had a metastatic regional LN were defined as belonging to the LN-positive group, and others were defined as being in the LN-negative group.

Table 1 shows the clinicopathologic characteristics of patients in the LN-positive group. The median age at the

time of diagnosis was 62 years (range 31–83). The male/female ratio was 1.0:0.9. Primary lesions were in the colon in 67 patients and in the rectum in 30 patients. Extracapsular LN involvement was detected in 47 patients. The liver metastases could be resected in 18 of the 47 patients. Tumors in the liver were synchronous with the primary tumor in 75 patients. Among them, synchronous resection of CRC liver metastases was performed in 25 patients. The others received chemotherapy (e.g., oxaliplatin+5-FU+leucovorin). Altogether, 46 patients had liver metastasis consisting of fewer than three lesions (ranging from one to uncountable). In all, 32 (33.0 %) patients presented with a solitary metastasis and 51 (52.6 %) with more than three. A total of 42 patients had a hepatic metastasis that was >3 cm. The distribution of liver metastases was bilobar in 48 (49.5 %) patients.

Extracapsular invasion

Of the 97 patients, ECI was found in 47 (48.5 %) and intracapsular LNs in 50 (51.5 %). ECI did not correlate with the sex of the patient ($p = 0.1303$), pT ($p = 0.6536$), lymphovascular invasion ($p = 0.0941$), or liver metastases >3 cm ($p = 0.5205$). A significant correlation was noted for the number of positive LNs (0.0022), the timing of development ($p = 0.0238$), and the number of liver metastases (0.0001). Among the 26 (74.3 %) patients with more than four liver metastases, ECI was detected in the regional LNs of those with primary CRC (Table 2).

During this study period, 47 patients who underwent hepatic resection for CRC metastases had regional LN metastasis from the CRC. The median age for hepatic resection was 61 years of age (range 31–83 years). The male/female ratio was 1.5:1.0. The primary cancer was rectal in origin in 18 (38.3 %) patients. The average number of positive LNs was 2.6, and ECI was detected in 18 patients. Synchronous hepatic metastases were present in 25 (53.2 %) patients, with 10 patients having more than three metastases. The median size of the largest hepatic metastases was 33.8 mm (range 10–120 mm). The distribution of liver metastases was bilobar in 10 (21.3 %) patients. A total of 7 patients received neoadjuvant chemotherapy, and 24 received adjuvant chemotherapy. The LN-negative group is also shown in Table 3. There was no statistical difference between the LN-positive and LN-negative groups (Table 3).

Univariate analysis of prognostic factors

A univariate analysis was performed to study the relation between the various factors and overall survival in patients who underwent liver resection with a metastatic regional LN. The sex and age of patients did not show statistically

Table 3 Patient characteristics after liver resection

Variable	LN-positive (n = 47)	LN-negative (n = 24)	<i>p</i>
Sex			0.3516
Male	28 (59.6 %)	17 (70.8 %)	
Female	19 (40.4 %)	7 (29.2 %)	
Age (years)	61 (31–83)	63 (41–81)	0.5274
Primary site			0.4461
Colon	29 (61.7 %)	17 (70.8 %)	
Rectum	18 (38.3 %)	7 (29.2 %)	
pT			0.0763
pT2	2 (4.3 %)	6 (25.0 %)	
pT3	6 (12.8 %)	16 (66.7 %)	
pT4	39 (83.0 %)	2 (8.3 %)	
No. of positive LNs	2.6 ± 1.8 (1–8)	0	
ECI			–
Positive	18 (38.3 %)	–	
Negative	29 (61.7 %)	–	
Histology			0.0512
Well differentiated	6 (12.8 %)	6 (25 %)	
Moderately differentiated	37 (78.7 %)	17 (70.8 %)	
Poorly differentiated/ mucinous	4 (8.5 %)	1 (4.2 %)	
Lymphovascular invasion			0.5613
Negative	21 (44.7 %)	10 (41.7 %)	
Positive	26 (55.3 %)	14 (58.3 %)	
Timing of development			0.2106
Metachronous	22 (46.8 %)	15 (62.5 %)	0.1085
Early	16 (34.0 %)	7 (29.2 %)	
Late	6 (12.8 %)	8 (33.3 %)	
Synchronous	25 (53.2 %)	9 (37.5 %)	
No. of metastases			0.5406
1–2	37 (78.2 %)	20 (83.3 %)	
≥3	10 (21.3 %)	4 (16.6 %)	
Maximum diameter (mm)	33.8 (10–120)	36.7 (15–130)	
Tumor distribution			0.3657
Unilateral	37 (78.7 %)	21 (87.5 %)	
Bilateral	10 (21.3 %)	3 (12.5 %)	
Extent of resection			0.2293
Major	14 (29.8 %)	5 (20.1 %)	
Minor	33 (70.2 %)	19 (79.3 %)	
Resection margin			0.1555
≥5 mm	25 (53.2 %)	16 (66.7 %)	
<5 mm	22 (46.8 %)	8 (33.3 %)	
Neoadjuvant			0.8451
Yes	7 (14.9 %)	4 (16.7 %)	
No	40 (85.1 %)	20 (83.3 %)	

Table 3 continued

Variable	LN-positive (n = 47)	LN-negative (n = 24)	<i>p</i>
Adjuvant			0.5613
Yes	24 (51.1 %)	14 (58.3 %)	
No	23 (48.9 %)	10 (41.7 %)	

significant differences concerning overall survival. The localization and pathologic T stage also did not show a statistically significant difference concerning survival after liver metastasis resection. In contrast, the number of positive LNs ($p = 0.0014$) and ECI ($p = 0.0203$) were significantly associated with overall survival. No statistically significant difference was found for survival of patients with multiple metastases compared to a single metastasis. Timing of metastasis, maximum diameter, and tumor distribution also showed no correlation in the patients with liver metastasis resection. The patients who received adjuvant chemotherapy had better overall survival rates ($p = 0.0423$), although the overall survival rates for patients who received neoadjuvant chemotherapy were similar—regardless of the sequence of treatment before or after surgery (Table 4). Results of the multivariable analyses are shown in Table 5. Only the number of positive LNs was an independent prognostic factor (hazard ratio 1.257, 95 % confidence interval 1.012–1.539, $p = 0.0388$).

The clinicopathologic characteristics of 18 patients with ECI and 29 patients with intracapsular LN involvement who underwent liver resection are summarized in Table 6. For all 47 patients, there were no significant differences in sex, tumor location, pathologic T stage, pathologic differentiation, LN status, number of liver metastases, timing of metastases, or tumor distribution of liver metastases between ECI and intracapsular LN involvement. However, the patients with ECI had a high propensity for recurrence after liver resection ($p = 0.0608$).

Prognosis

Kaplan–Meier survival curves illustrate survival after liver resection in patients whose primary tumor was associated with regional LN metastases. In the patients who underwent liver resection, overall survival rates were 91.2 % at 1 year, 69.8 % at 3 years, and 46.9 % at 5 years (Fig. 2). Figure 3 shows the comparison between the LN-positive group and the LN-negative group in patients with a liver resection. There was a statistical difference between the two groups ($p = 0.0363$). To assess whether the prognostic difference in these patients was different from extracapsular LN involvement, the positive group was divided into

Table 4 Univariate analysis of overall survival after curative resection of liver metastases (LN-positive)

Variables	No.	Survival		<i>p</i>
		5-Year (%)	Median (months)	
Sex				
Male	28	39.2	58.9	0.4999
Female	19	52.0	64.1	
Age (years)				
<65	30	49.8	58.0	0.6857
≥65	17	44.5	48.6	
Primary site				
Colon	29	57.5	51.9	0.0998
Rectum	18	24.0	42.4	
pT				
pT1–pT3	42	50.9	65.4	0.0531
pT4	5	20.0	33.8	
No. of positive LNs				
1–2	26	67.9	54.3	0.0014
>2	21	29.5	39.6	
ECI				
Positive	18	18.2	38.8	0.0203
Negative	29	57.2	52.9	
Histology				
Well/mod. differentiated	38	47.4	46.0	0.2988
Poorly differentiated/mucinous	9	62.5	32.0	
Lymphovascular invasion				
Negative	18	40.5	47.5	0.6218
Positive	29	46.0	65.4	
Timing of development				
Metachronous	22	55.3	65.4	0.2238
Early	16	54.7	64.1	0.1521
Late	6	80.0	–	
Synchronous	25	39.3	44.2	
No. of metastases				
Single	26	49.7	65.4	0.4975
Multiple	21	36.7	58.9	
Maximum diameter				
<4 cm	33	45.5	65.4	0.211
≥4 cm	14	25.8	48.0	
Tumor distribution				
Unilateral	37	41.7	58.9	0.842
Bilateral	10	50.0	65.4	
Extent of resection				
Major	14	35.6	58.9	0.4195
Minor	33	47.4	65.4	
Resection margin				
≥5 mm	24	43.0	65.4	0.7034
<5 mm	23	41.0	48.0	

Table 4 continued

Variables	No.	Survival		<i>p</i>
		5-Year (%)	Median (months)	
Neoadjuvant				0.7273
Yes	7	37.5	54.9	
No	40	47.6	53.5	
Adjuvant				0.0423
Yes	24	62.7	179.0	
No	23	28.1	39.2	

Table 5 Multivariate analysis of overall survival after curative resection of liver metastases (LN-positive)

Variable	HR	95 % CI	<i>p</i>
No. of positive LNs	1.257	1.012–1.539	0.0388
ECI	1.513	0.966–2.360	0.0700
Adjuvant	0.701	0.414–1.110	0.1398

HR hazard ratio, CI confidence interval

two groups: an ECI-positive group and an ECI-negative group. No difference in overall survival was observed between LN-negative patients and ECI-negative patients, whereas the ECI-positive patients had a significantly poorer prognosis than the other two groups ($p = 0.0024$) (Fig. 4).

Discussion

It has been reported that extranodal invasion is an indicator of distant metastasis in patients with head, neck, prostate, and laryngeal cancers [21, 24, 25]. Concerning gastrointestinal cancers, it has also been reported that extranodal invasion indicates a poor prognosis and a risk of local recurrence in patients with rectal cancer [26]. In the present study, ECI at regional LNs is also associated with a worse outcome in CRC patients after resection of liver metastases.

Upto 50 % of patients with resected liver metastases develop recurrence of neoplastic disease [14, 27]. In our study, poorer overall survival was significantly associated with the number of positive LNs and ECI. There have been several reports on the risk factors after hepatic resection for metastatic colon cancer. A number of risk factors have been consistently reported as important in predicting a poorer outcome following hepatic resection of metastatic colon cancer, including the number and size of hepatic metastases, distribution of tumors, involved resection

Table 6 Association between clinicopathologic characteristics and ECI after liver resection

Variable	ECI-positive (n = 18)	ECI-negative (n = 29)	p
Sex			0.8657
Male	11	17	
Female	7	12	
Age (years)			0.0284
<65	15	15	
≥65	3	14	
Primary site			0.3476
Colon	11	18	
Rectum	7	11	
pT			0.9340
pT1–pT3	16	26	
pT4	2	3	
No. of positive LNs			0.0735
1–2	11	10	
>2	7	19	
Histology			0.7333
Well/mod. differentiated	15	23	
Poorly differentiated/mucinous	3	6	
Lymphovascular invasion			0.2777
Negative	7	16	
Positive	11	13	
Timing of development			0.1447
Metachronous	6	16	
Early	4	12	
Late	2	4	
Synchronous	12	13	
No. of metastases			0.6192
1–3	16	27	
≥4	2	2	
Maximum diameter			0.6765
<4 cm	12	21	
≥4 cm	6	8	
Tumor distribution			0.5429
Unilateral	15	22	
Bilateral	3	7	
Recurrence			0.1055
Positive	13	15	
Negative	5	14	
Chemotherapy			0.1870
Yes	7	17	
No	11	12	

margin, synchronous disease, CEA level, and LN-positive primary tumor [10, 12–19]. Malik et al. [28] developed a preoperative scoring system following analysis of 687

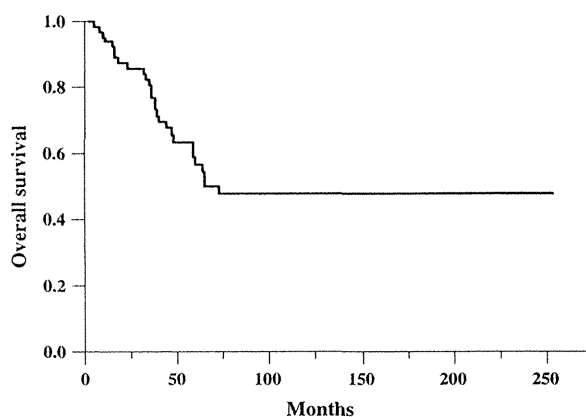


Fig. 2 Overall survival of patients with colorectal liver metastasis after liver resection

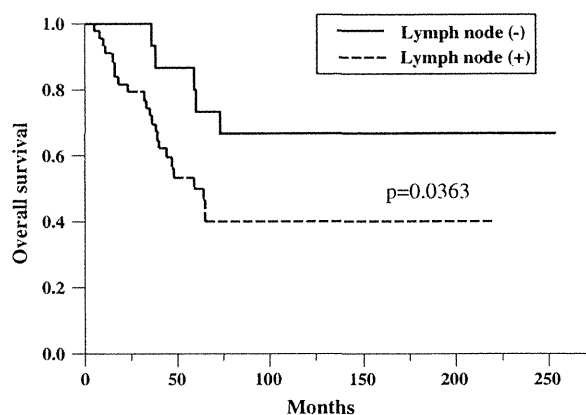


Fig. 3 Overall survival of the LN-positive and LN-negative groups of patients with colorectal liver metastasis after liver resection ($p = 0.0363$)

patients who underwent resection of colorectal liver metastases over a period of 13 years. In their study, the number of metastases and an inflammatory response to tumors were independent predictors of poorer disease-free and overall survival. Konopke et al. [29] published a suggestive prognostic scoring system in 2009 following prospective analysis of 201 patients referred to their institution over 13 years. Multivariable analysis revealed synchronous colorectal primary and liver metastases, the presence of four or more liver metastases, and CEA > 200 ng/ml as adverse prognostic factors. However accurate statistical analysis may be, it does not mean that data or a prognostic model from one institution will fit into another institution’s data set addressing the same disease. Invariably, selection biases, population differences, differences in groups of variables, differences in length of follow-up, interpretation

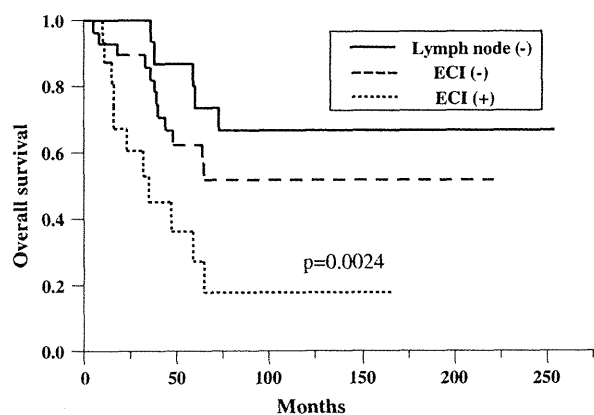


Fig. 4 Overall survival of the LN-negative group and extracapsular invasion (ECI) in the regional LNs in patients with colorectal liver metastasis after liver resection. There were significant differences between patients in the ECI-positive group and those in the other two groups ($p = 0.0024$)

of radiologic imaging, and improvements in surgical techniques come into play.

The number of liver metastases was well recognized as a prognostic factor. Nordlinger et al. [17] observed that having more than four liver metastases was a significant prognostic factor. Malik et al. [28] also showed that the presence of eight or more liver metastases and an inflammatory response to tumors were independent predictors in a multivariable analysis. In our study, the number of colorectal liver metastases was closely related to ECI in patients, including those with resectable and unresectable liver metastases. However, it is not correlated with overall survival in patients of colorectal liver metastases after resection. The reason is that ECI may represent only aggressive biologic behavior. Most of our patients who underwent liver resection had fewer than three liver metastases. If we had tried to perform liver resection aggressively in patients with multiple liver metastases (more than four), the overall survival rates for those who had ECI would have been worse than for those without ECI.

With respect to neoadjuvant chemotherapy, no trial has established a role for giving it preoperatively. However, the response to neoadjuvant therapy before liver resection is important for outcome. Some authors have reported that response to neoadjuvant chemotherapy was not related to overall survival. However, Gruenberger et al. [9] reported that response to neoadjuvant oxaliplatin-based chemotherapy positively influenced achieving a better prognosis when liver resection was performed after it. Moreover, Adam et al. [7, 8] reported that lack of response to neoadjuvant chemotherapy for resectable liver metastasis is associated with a shorter survival. The majority of patients

who undergo hepatic resection secondary to neoadjuvant chemotherapy experienced disease recurrence. In our study, patients who were given neoadjuvant chemotherapy did not have better prognoses. Most of our patients with neoadjuvant therapy had liver metastasis that was initially unresectable. Disappointingly, the majority of patients experienced disease recurrence within several months.

Careful patient selection might be one of the most important factors for prolonging disease-free survival after hepatectomy. In regard to adjuvant chemotherapy, however, the meta-analysis showed the benefit of adjuvant chemotherapy when treating those with resectable colorectal liver metastasis. Thus, postoperative systematic chemotherapy should be performed [30]. In our experience, the use of systemic adjuvant chemotherapy after potentially curative resection of metastases from CRC was associated with better overall survival ($p = 0.0423$). However, adjuvant chemotherapy is sometimes difficult after hepatectomy. The patient's safety during adjuvant chemotherapy after hepatectomy should remain the priority. In Japan, a clinical trial investigating the safety data of the adjuvant FOLFOX focusing on allergic reactions and peripheral sensory neuropathy is proceeding.

Involvement of a number of regional LNs from the primary CRC was a prognostic factor of poor outcome in our study. In various other studies, involvement of regional LNs from primary CRCs has been shown to be a significant prognostic factor for outcome in patients undergoing hepatic resection. By employing a nomogram for estimating survival in patients with colorectal liver metastases, Kattan et al. [19] showed that an increase in the number of metastatic regional LNs was related to a worse outcome. Kanemitsu and Kato [18], using pretreatment and post-treatment prognostic nomograms for a retrospective analysis of 578 patients with hepatic metastases from CRC, showed that the number of LNs associated with the primary lesion was one of the independent adverse prognostic variables.

The extent of lymphatic dissemination is one of the most important predictors for survival in cancer patients. However, the relation between lymphangiogenesis and hematogenous dissemination that leads to liver metastases remains unclear. It could be hypothesized that tumor cell metastases obstruct efferent lymphatics, causing occlusion. It has been reported that lymphatic obstruction resulting in aberrant flow of lymph fluid leads to lymphovenous communication and, consequently, hematogenous dissemination [31]. Based on these phenomena, Kumagai et al. [32] suggested that tumor cell obstruction in the lymph system would lead to liver metastases in the digestive organs. Extranodal invasion may indicate the elevation of endolymphatic pressure. Therefore, we believe that there is a strong relation between ECI and liver metastases of CRC.

In this study, we were able to identify patients who appear to have biologically more aggressive tumors given that survival was significantly reduced with the presence of ECI in the regional LN metastases from primary CRC. Some authors have suggested that when ECI permits a tumor to break through the LN capsule the tumor may be highly aggressive. For gastric carcinoma, Alakus et al. [33] reported that once the capsules of the LNs had been penetrated by tumor tissue, the chance of cure by surgery was minimal.

The most important finding was that there was a significantly lower survival rate for the patient group with ECI in the regional LNs than in the other groups after resection of colorectal liver metastases. These results indicate that CRC with ECI at the regional LNs is characterized by a more aggressive tumor, with respect to a biologic point of view. Liver metastases with ECI also fit with the concept of this more aggressive behavior. Therefore, ECI at the regional LNs may represent more micrometastases with a higher tendency to spread, which may lead to earlier recurrence and a worse prognosis.

Despite these encouraging results, the present study has some limitations. The number of patients included was limited. Also, at present the follow-up has continued for only 32 months. Therefore, it is difficult to draw definitive conclusions about ECI. Larger trials with a longer follow-up are needed to clarify the usefulness of ECI as a predictor in patients with colorectal liver metastasis.

References

- Fernandez FG, Drebin JA, Linehan DC et al (2004) Five-year survival after resection of hepatic metastases from colorectal cancer in patients screened by positron emission tomography with F-18 fluorodeoxyglucose (FDG-PET). *Ann Surg* 240:438–447 discussion 447–450
- Gomez D, Morris-Stiff G, Wyatt J et al (2008) Surgical technique and systemic inflammation influence long-term disease-free survival following hepatic resection for colorectal metastasis. *J Surg Oncol* 98:371–376
- Tomlinson JS, Jarnagin WR, DeMatteo RP et al (2007) Actual 10-year survival after resection of colorectal liver metastases defines cure. *J Clin Oncol* 25:4575–4580
- De Haas RJ, Adam R, Wicherts DA et al (2010) Comparison of simultaneous or delayed liver surgery for limited synchronous colorectal metastases. *Br J Surg* 97:1279–1289
- Lambert LA, Colacchio TA, Barth RJ Jr (2000) Interval hepatic resection of colorectal metastases improves patient selection. *Arch Surg* 135:473–479 discussion 479–480
- Yoshidome H, Kimura F, Shimizu H et al (2008) Interval period tumor progression: does delayed hepatectomy detect occult metastases in synchronous colorectal liver metastases? *J Gastrointest Surg* 12:1391–1398
- Adam R, Pascal G, Castaing D et al (2004) Tumor progression while on chemotherapy: a contraindication to liver resection for multiple colorectal metastases? *Ann Surg* 240:1052–1061
- Adam R, Wicherts DA, de Haas RJ et al (2008) Complete pathologic response after preoperative chemotherapy for colorectal liver metastases: myth or reality? *J Clin Oncol* 26:1635–1641
- Gruenberger B, Scheithauer W, Punzengruber R et al (2008) Importance of response to neoadjuvant chemotherapy in potentially curable colorectal cancer liver metastases. *BMC Cancer* 8:120
- Arru M, Aldrighetti L, Castoldi R et al (2008) Analysis of prognostic factors influencing long-term survival after hepatic resection for metastatic colorectal cancer. *World J Surg* 32:93–103
- Choti MA, Sitzmann JV, Tiburi MF et al (2002) Trends in long-term survival following liver resection for hepatic colorectal metastases. *Ann Surg* 235:759–766
- Fong Y, Fortner J, Sun RL et al (1999) Clinical score for predicting recurrence after hepatic resection for metastatic colorectal cancer: analysis of 1001 consecutive cases. *Ann Surg* 230:309–318 discussion 318–321
- Kanas GP, Taylor A, Primrose JN et al (2012) Survival after liver resection in metastatic colorectal cancer: review and meta-analysis of prognostic factors. *Clin Epidemiol* 4:283–301
- Rees M, Tekkis PP, Welsh FK et al (2008) Evaluation of long-term survival after hepatic resection for metastatic colorectal cancer: a multifactorial model of 929 patients. *Ann Surg* 247:125–135
- Settmacher U, Dittmar Y, Knosel T et al (2011) Predictors of long-term survival in patients with colorectal liver metastases: a single center study and review of the literature. *Int J Colorectal Dis* 26:967–981
- Jaecq D, Bachellier P, Guiguet M et al (1997) Long-term survival following resection of colorectal hepatic metastases. *Association Francaise de Chirurgie. Br J Surg* 84:977–980
- Nordlinger B, Guiguet M, Vaillant JC et al (1996) Surgical resection of colorectal carcinoma metastases to the liver: a prognostic scoring system to improve case selection, based on 1,568 patients. *Association Francaise de Chirurgie. Cancer* 77:1254–1262
- Kanemitsu Y, Kato T (2008) Prognostic models for predicting death after hepatectomy in individuals with hepatic metastases from colorectal cancer. *World J Surg* 32:1097–1107
- Kattan MW, Gonen M, Jarnagin WR et al (2008) A nomogram for predicting disease-specific survival after hepatic resection for metastatic colorectal cancer. *Ann Surg* 247:282–287
- Ishida T, Tateishi M, Kaneko S et al (1990) Surgical treatment of patients with nonsmall-cell lung cancer and mediastinal LN involvement. *J Surg Oncol* 43:161–166
- Mikel Hubanks J, Boorjian SA, Frank I et al (2013) The presence of extracapsular extension is associated with an increased risk of death from prostate cancer after radical prostatectomy for patients with seminal vesicle invasion and negative LNs. *Urol Oncol* 32(26):e1–e7
- Stitzenberg KB, Meyer AA, Stern SL et al (2003) Extracapsular extension of the sentinel LN metastasis: a predictor of nonsentinel node tumor burden. *Ann Surg* 237:607–612
- Fujii T, Tabe Y, Yajima R et al (2011) Process of distant LN metastasis in colorectal carcinoma: implication of extracapsular invasion of LN metastasis. *BMC Cancer* 11:216
- Alvi A, Johnson JT (1997) Development of distant metastasis after treatment of advanced-stage head and neck cancer. *Head Neck* 19:500–505
- Oosterkamp S, de Jong JM, Van den Ende PL et al (2006) Predictive value of LN metastases and extracapsular extension for the risk of distant metastases in laryngeal carcinoma. *Laryngoscope* 116:2067–2070
- Heide J, Krull A, Berger J (2004) Extracapsular spread of nodal metastasis as a prognostic factor in rectal cancer. *Int J Radiat Oncol Biol Phys* 58:773–778

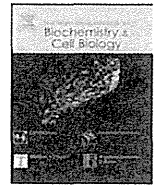
27. Aloia TA, Vauthey JN, Loyer EM et al (2006) Solitary colorectal liver metastasis: resection determines outcome. *Arch Surg* 141:460–466 discussion 466–467
28. Malik HZ, Prasad KR, Halazun KJ et al (2007) Preoperative prognostic score for predicting survival after hepatic resection for colorectal liver metastases. *Ann Surg* 246:806–814
29. Konopke R, Kersting S, Distler M et al (2009) Prognostic factors and evaluation of a clinical score for predicting survival after resection of colorectal liver metastases. *Liver Int* 29:89–102
30. Mitry E, Fields AL, Bleiberg H et al (2008) Adjuvant chemotherapy after potentially curative resection of metastases from colorectal cancer: a pooled analysis of two randomized trials. *J Clin Oncol* 26:4906–4911
31. Allen PJ, Kemeny N, Jarnagin W et al (2003) Importance of response to neoadjuvant chemotherapy in patients undergoing resection of synchronous colorectal liver metastases. *J Gastrointest Surg* 7:109–115 discussion 116–117
32. Kumagai K, Shimizu K, Yokoyama N et al (2010) Gastrointestinal cancer metastasis and lymphatic advancement. *Surg Today* 40:301–306
33. Alakus H, Holscher AH, Grass G et al (2010) Extracapsular LN spread: a new prognostic factor in gastric cancer. *Cancer* 116:309–315

松本 美佐子
(北海道大学)



Contents lists available at ScienceDirect

The International Journal of Biochemistry & Cell Biology

journal homepage: www.elsevier.com/locate/biociel

Cells in focus

Dendritic cell subsets involved in type I IFN induction in mouse measles virus infection models

Hiromi Takaki*, Hiroyuki Oshiumi, Misako Matsumoto, Tsukasa Seya*

Department of Microbiology and Immunology, Hokkaido University Graduate School of Medicine, Kita-ku, Sapporo 060-8638, Japan

ARTICLE INFO

Article history:

Received 20 March 2014

Received in revised form 28 April 2014

Accepted 1 May 2014

Available online 4 June 2014

Keywords:

Dendritic cells

Measles virus

Mouse model

Type I interferon (IFN)

Immune suppression

ABSTRACT

Measles caused by measles virus (MV) infection remains important in child mortality. Although the natural host of MV is human, mouse models expressing MV entry receptors (human CD46, CD150) and disrupting the interferon (IFN) pathways work for investigating immune responses during early MV infection *in vivo*. Dendritic cells (DCs) are primary targets for MV in the mouse models and are efficiently infected with several MV strains in the respiratory tract *in vivo*. However, questions remain about what kind of DC in a variety of DC subsets is involved in initial MV infection and how the RNA sensors evoke circumventing signals against MV in infected DCs. Since type I IFN-inducing pathways are a pivotal defense system that leads to the restriction of systemic viral infection, we have generated CD150-transgenic mice with disrupting each of the IFN-inducing pathway, and clarified that DC subsets had subset-specific IFN-inducing systems, which critically determined the DC's differential susceptibility to MV.

© 2014 Elsevier Ltd. All rights reserved.

1. Introduction

The pathogenic measles virus (MV) causes measles in infants. The MV genome is a nonsegmented negative single-stranded RNA consisting of six genes that encode the nucleocapsid (N), phosphoprotein (P), matrix (M), fusion (F), hemagglutinin (H), and large (L) proteins. The P gene encodes P protein and the nonstructural V and C proteins. Although the nonstructural V and C proteins of wild type (WT) strains of MV are important in suppressing the host interferon (IFN) response in human cells (Gerlier and Valentin, 2009), WT strains of MV are less able to suppress type I IFN production in murine cells than in human cells (Shingai et al., 2005), suggesting that V and C proteins are relatively ineffective suppressors for IFN response in murine cells.

CD46 (also called MCP) was first identified as an MV entry receptor for laboratory-adapted and vaccine strains of MV. CD46 is expressed in all human nucleated cells including epithelial cells (Gerlier and Valentin, 2009). In 2000, human CD150, a signaling lymphocyte activation molecule (SLAM), was identified as the second MV entry receptor for all MV strains including WT (Tatsuo et al., 2000). Expression of CD150 is restricted to activated lymphocytes,

dendritic cells (DCs), and macrophages (Delpeut et al., 2012), consistent with the lymphotropism of MV. However, the expression pattern of CD150 does not explain why WT strains of MV infect epithelial cells that do not express CD150. Recently, human nectin-4 (also called poliovirus receptor-related 4, PVRL4) was identified as the third entry receptor for WT strains of MV (Mühlebach et al., 2011; Noyce et al., 2011). Expression of nectin-4 is restricted to the basolateral surface of epithelial cells (Delpeut et al., 2012). Thus, laboratory-adapted and vaccine strains of MV use CD46 and CD150 as entry receptors, and WT strains of MV use CD150 and nectin-4. Initial infection with WT strains of MV *via* CD150 occurs in DCs and alveolar macrophages (AMs) and secondary spreading of MV infection is established in lymphocytes through infected DCs and AMs. Ultimately, MV-infected lymphocytes systemically spread to distal sites including the respiratory tract and then MV infects epithelial cells *via* nectin-4, resulting in release of MV into the airway lumen of the infected lung (Delpeut et al., 2012). C-type lectin DC-SIGN (also called CD209) has an important role for infection of DCs by laboratory-adapted and WT strains of MV (de Witte et al., 2006), although DC-SIGN is dispensable for MV entry. Both attachment and infection of immature DCs with MV are blocked by DC-SIGN inhibitors, suggesting that DC-SIGN is critical for enhancement of CD46/CD150-mediated infection of DCs (de Witte et al., 2006).

Human CD150 transgenic (Tg) and CD150 knock-in mice were generated as MV infection models to study receptor tropism and the immune dynamics of MV (Hahm et al., 2003, 2004; Ohno et al., 2007; Sellin et al., 2006; Shingai et al., 2005; Welstead et al., 2005) and these mice were somehow permissive to MV *in vivo*.

* Corresponding authors at: Department of Microbiology and Immunology, Hokkaido University Graduate School of Medicine, Kita 15, Nishi 7, Kita-ku, Sapporo 060-8638, Japan. Tel.: +81 11 706 7866; fax: +81 11 706 7866.

E-mail addresses: tahiro@sci.hokudai.ac.jp (H. Takaki), seya-tu@pop.med.hokudai.ac.jp (T. Seya).

Systemic infection by WT strains of MV *in vivo* was observed in CD150Tg/*Irfnar1*^{-/-} mice, generated by crossing CD150Tg mice with mice having the disrupted IFN receptor 1 (*Irfnar*) gene; the other is CD150Tg/*Stat1*^{-/-} mice, generated by crossing CD150Tg mice with mice knocked out for the signal transduction and activator of transcription 1 (*Stat1*) gene, which is a major signaling molecule for the IFN receptor (Shingai et al., 2005; Welstead et al., 2005). Both models indicate the importance of the IFNAR pathway for restricting MV *in vivo* infection in mice. DCs and AMs are primary targets for MV intranasally inoculated into CD150Tg models (Ferreira et al., 2010), since these cells express CD150 and are located in the lung where host cells firstly encounter MV. Results from mouse models for MV *in vivo* infection reflect *in vitro* high susceptibility of human monocyte-derived DCs (moDCs) to MV. DCs and AMs are the first target cells during early MV infection in monkeys (de Swart et al., 2007; Lemon et al., 2011). All these data indicate that type I IFN produced by DCs and AMs primarily protects hosts from systemic MV infection.

In this review, we summarized the mouse model studies on the host antiviral response to MV infection, which involves both toll-like receptors (TLRs) and retinoic acid-inducible gene (RIG)-I-like receptors (RLRs) in specific DC subsets.

2. Type I IFN-inducing pathways respond to viral RNA

The IFN response, which is the induction of type I IFN- α/β is a major antiviral defense pathway that confers virus resistance to neighboring cells. Previous reports showed that viral RNA is detected by cytoplasmic pattern recognition receptors (PRRs) such as RIG-I and the melanoma differentiation-associated gene 5 (MDA5) (Kawai and Akira, 2009). MDA5 and RIG-I detect long and short dsRNA, respectively (Kato et al., 2008). TLR3 recognizes extracellular double-stranded RNA (dsRNA) in the endosome whereas RIG-I and MDA5 sense cytoplasmic dsRNA (Fig. 1). TLR3 recruits the adaptor, Toll/interleukin-1 receptor (TIR) homology domain-containing adaptor molecule 1 (TICAM-1, also called TRIF) in response to dsRNA and induces type I IFN production. Activation of RLRs is regulated by multiple consecutive processes including dephosphorylation, ubiquitination and oligomerization of RLR (Gack et al., 2007; Wies et al., 2013). The CARD domain of RLRs is phosphorylated by unknown kinases in steady state, prohibiting RLR activation (Wies et al., 2013). Viral infection activates RLRs via dephosphorylation by serine-threonine phosphatases PP1 α and PP1 γ (Wies et al., 2013). The dephosphorylated RLRs provide signals through the mitochondrial antiviral signaling protein (MAVS; also called VISA, Cardif, or IPS-1) to induce type I IFN. Disrupting these adaptor genes results in failure to activate IFN regulatory factor (IRF)-3 and IRF-7, abrogating type I IFN production and antiviral host defense. Virus-derived single-stranded RNA (ssRNA) is recognized by TLR7 and TLR8 which are in the endosome. MyD88-dependent signaling is activated upon viral RNA recognition by TLR7 to induce type I IFNs (Kawai and Akira, 2009). Unlike ubiquitously expressed RLRs, TLR expression is restricted to particular cell types with a different set of TLRs (Table 1) (Edwards et al., 2003). This differential expression pattern of TLRs directs specific sets of cells to respond to particular TLR ligands, which enhance a variety of immune responses.

3. Type I IFN induction in MV-infected murine DCs

Studies in mice with targeted gene deletions provide insight into the mechanisms of type I IFN induction in response to MV infection *in vivo* and *in vitro*. Bone marrow-derived DCs (BMDCs) were used to study MV permissiveness of DCs, initially in CD150Tg mice (Ohno et al., 2007; Shingai et al., 2005; Welstead et al., 2005).

Studies using BMDCs from CD150Tg mice in combination with *Mavs*^{-/-}, *Irf3*^{-/-}/*Irf7*^{-/-}, *Ticam1*^{-/-} and *Myd88*^{-/-} mice showed that type I IFN expression in BMDCs completely relied on MAVS but not TICAM-1 and MyD88 (Takaki et al., 2014). Surprisingly, BMDCs derived from CD150Tg/*Irf3*^{-/-}/*Irf7*^{-/-} mice produce a detectable IFN- β in response to MV infection, which confers nonpermissiveness to CD150Tg/*Irf3*^{-/-}/*Irf7*^{-/-} BMDCs (Takaki et al., 2014). A pharmacological study indicated that MV-derived IFN- β expression partially depended on NF- κ B (Takaki et al., 2014). A recent study using West Nile virus showed that IRF3/IRF7 and IRF5 coordinately regulate the type I IFN response in DCs (Lazear et al., 2013). For MV, IRF5 might be a transcription factor for MAVS-dependent and IRF3/IRF7-independent type I IFN induction in BMDCs (Fig. 2).

An *in vivo* MV infection study using a CD150Tg mouse model revealed that MAVS disruption scarcely led MV permissiveness or type I IFN gene expression in the spleen compared to CD150Tg mice (Takaki et al., 2013). *In vitro* infection assays showed that isolated cell subsets of CD11c⁺ DCs, but not T or B cells, mainly produced type I IFN in response to MV infection through a MAVS-independent pathway. Various types of DCs have been identified in mouse secondary lymphoid tissues, including three CD11^{high} subsets of conventional DCs (cDCs): CD8 α ⁺, CD4⁺ and CD4⁻ CD8 α ⁻ double negative (DN) DCs (Vremec et al., 2000), and one subset of CD11c^{low} plasmacytoid DCs (pDCs) (Asselin-Paturel et al., 2001). These DC subsets express different sets of TLR genes and have distinct functions (Table 1) (Edwards et al., 2003; Luber et al., 2010). Mouse pDCs express most TLRs except TLR3 and therefore respond to a wide range of pathogen-associated molecular patterns including TLR7 ligand (Boonstra et al., 2003; Edwards et al., 2003). CD8 α ⁺ DCs express high amounts of TLR3, but not TLR7 (Edwards et al., 2003) and mainly participate in poly I:C-induced cross-presentation. Although a CD4⁺ and DN DCs have a similar TLR expression pattern (Edwards et al., 2003), CD4⁺ DCs but not DN DCs express TLR7 protein at low levels (Takaki et al., 2013). Type I IFN expression is induced in CD4⁺ DCs and pDCs, but not CD8 α ⁺ and DN DCs that are isolated from MAVS-disrupted mice during *in vitro* MV infection (Takaki et al., 2013). This result indicates that type I IFN-inducing pathways in pDC and CD4⁺ DCs are independent of the MAVS pathway. A pharmacological study showed that the MyD88 pathway is involved in a MAVS-independent type I IFN-inducing pathway (Takaki et al., 2013). This result was confirmed using CD150Tg/*Myd88*^{-/-} pDCs, suggesting that TLR7 is responsible for recognition of MV RNA in CD4⁺ and pDCs. Since the RLR-MAVS pathway usually senses endogenous viral RNA in CD4⁺ DCs (Luber et al., 2010), MAVS disruption highlights that the MyD88 pathway participates in initial type I IFN induction in CD4⁺ DCs in MV infection (Fig. 2). However, CD150Tg/*Myd88*^{-/-} mice are not permissive to MV infection *in vivo*, both MyD88 in pDCs and CD4⁺ DCs and MAVS in other cells contribute to protection against systemic MV infection.

Since TLR7 is in the endosome, viral RNA transport to the endosome is required to activate the TLR7/MyD88 pathway. Autophagy is required for the recognition of vesicular stomatitis virus by TLR7 to transport cytosolic viral replication intermediates into the lysosome, leading to type I IFN production in pDCs (Lee et al., 2007) IFN- β mRNA expression is induced in UV-irradiated MV-infected CD150Tg/*Mavs*^{-/-} DCs; however, treatment with an autophagy inhibitor prevented this IFN- β induction (unpublished data). These data suggest that autophagy but not viral replication is required for MV-mediated type I IFN induction via TLR7 in MAVS-disrupted murine DCs.

In contrast to BMDCs, type I IFN gene expression is observed in DCs and splenocytes derived from MV-infected CD150Tg/*Mavs*^{-/-} mice, which prevents DCs from MV infection *in vivo* in these mice (Takaki et al., 2013, 2014). RIG-I/MAVS but not TLR7/MyD88 mediates the antiviral response to RNA virus in conventional DCs. The

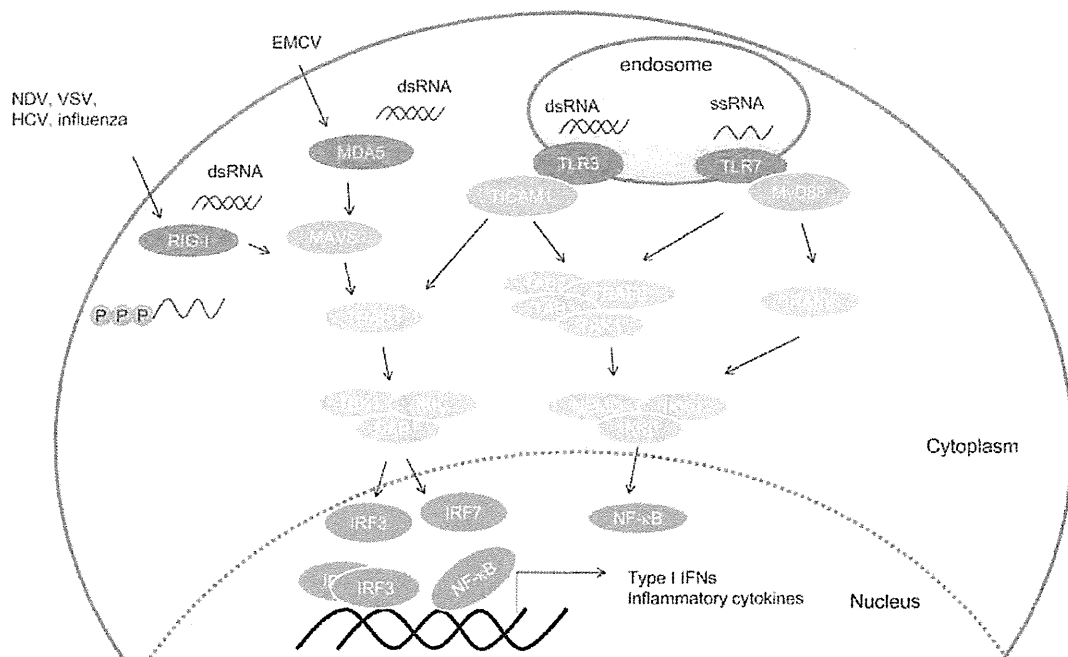


Fig. 1. Recognition of RNA by RLRs and TLRs. Double-stranded RNA (dsRNA) synthesized by RNA virus replication in infected cells is recognized by endosomal TLR3 and cytosolic RIG-I like receptors (RLRs), RIG-I and MDA5. They differentially recognize viral dsRNA products such that long dsRNA chains fit in MDA5, 5'-triphosphates short dsRNA couple with RIG-I and structured RNA activate TLR3 (Tatematsu et al., 2013). The outline of their signaling cascades that lead to the activation of IRF3 and NF-κB is overviewed (Kawai and Akira, 2009). Single-stranded RNA (ssRNA) is recognized by endosomal TLR7, leading to the activation of NF-κB and IKK α/β via adaptor protein MyD88. Transcription factor activation results in expression of type I IFN and inflammatory cytokines. NDV, newcastle disease virus; SeV, sendai virus; HCV, hepatitis C; EMCV, encephalomyocarditis virus

Table 1
Expression of TLRs in murine and human DC subset.

			TLR1	TLR2	TLR3	TLR4	TLR5	TLR6	TLR7	TLR8	TLR9	TLR10
Mouse	Conventional DCs (CD11c ^{high} B220 ⁻)	CD4 ⁺	+	+	-	+	+	+	+	-	+	-
		CD4 ⁻ CD8α ⁻	+	+	+/-	+	+	+	+/-	-	+	-
		CD4 ⁻	+	+	+	+	-	+	-	-	+	-
	Plasmacytoid DCs (CD11c ^{low} B220 ⁺ PDCA-1 ⁺)		+	+	-	+	+/-	+	+	-	+	-
Human	Myeloid DCs (CD11c ⁺)	Monocyte-derived DCs (moDCs)	+	+	+	+	+	+	+	+/-	-	+
		Plasmacytoid DCs (CD11c ⁻ BDCA2 ⁺ BDCA4 ⁺)	+/-	-	-	-	-	-	+	-	+	+

TLR expression in murine and human DC subset is described in refs (Jarrossay et al., 2001; Kadowaki et al., 2001; Edwards et al., 2003; Lubber et al., 2010).

studies using reporter mouse that expresses green fluorescence protein (GFP) under the control of the *Irf1-α6* promoter show that intranasal infection with newcastle disease virus (NDV) induces GFP expression in AMs and cDCs in lung as an initial defense via the RLR pathway (Kumagai et al., 2007). Although systemic NDV infection leads to GFP expression in not only pDCs but also cDCs and AMs, the frequency of GFP positive cells is higher in pDCs than in other cells. Thus, the activation of different subsets of DCs would be important to produce type I IFNs in systemic and local RNA virus infection.

Similar to murine DCs, PRRs expression differs with subsets of human DCs (Table 1) (Jarrossay et al., 2001; Kadowaki et al., 2001). In cDCs, MV transcription is required to activate type I IFN response, since UV-irradiated MV is unable to promote IFN-β production (Duhon et al., 2010). Type I IFN induction by pDCs depends on the recognition of MV RNA via the endosomal pathway, since UV-irradiated MV infection induces IFN-α production and this induction is cancelled by an endosomal acidification inhibitor in pDCs (Duhon et al., 2010). Although MV can inhibit TLR7 and TLR9-mediated type I IFN induction by MV-V and MV-C proteins in human pDCs (Pfaller and Conzelmann, 2008; Schlender et al., 2005; Yamaguchi et al., 2014), it remains unknown whether MV

proteins act as suppressors in murine DCs. Moreover, MV interacts with human DC-SIGN to enhance infection of human DCs (de Witte et al., 2006). However, how MV-H protein binds murine CIRE/DC-SIGN is unknown. The findings in murine DCs may differ from those in human DCs when infected with MV.

4. Type I IFN and cytokines in the context of MV immunosuppression

DCs contribute to MV-induced immunosuppression, including downregulation of costimulatory molecules and inhibition of IL-12 production following lipopolysaccharide stimulation (Coughlin et al., 2013; Hahm et al., 2004, 2007). MV infection suppressed BMDCs development via type I IFN that acts through STAT2-dependent signaling but independent of the STAT1 signaling (Hahm et al., 2005). Furthermore, *in vivo* MV infection induces a T helper type 2 response, enhances apoptosis, and induces regulatory T cells (Koga et al., 2010; Sellin et al., 2009). Blocking IL-10 signaling prevents MV-induced immunosuppression in CD150 knock-in mice, indicating that IL-10 participates in immunosuppression (Koga et al., 2010). In addition, high amounts of IL-10 are produced in CD4⁺ T cells obtained from MV-infected CD150Tg mice (Takaki

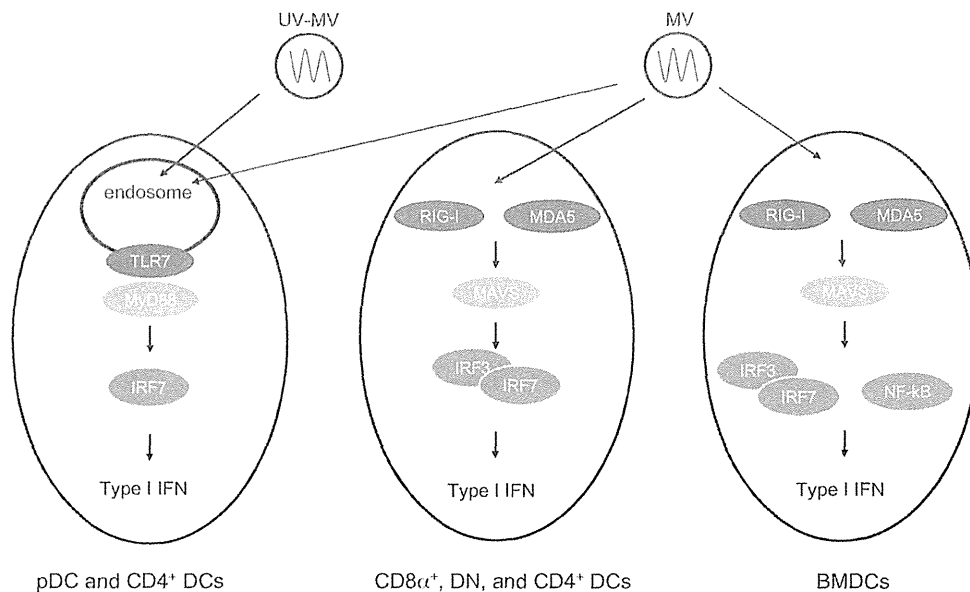


Fig. 2. Recognition of MV RNA in mouse DC subsets. DC subsets have their own viral RNA sensors to induce type I IFN. MV specifically infects these DC subsets. The ways for IFN induction in each DC subset are shown schematically. UV-MV; UV-irradiated MV

et al., 2014). In early infection by lymphocytic choriomeningitis virus (LCMV), type I IFN is produced via the TLR7/MyD88 pathway in pDCs. MDA5/MAVS-mediated type I IFN induction in other cells is required for sustained type I IFN responses to acute and chronic LCMV infection (Wang et al., 2012). Thus, different sources of type I IFN and signaling pathways affect immune responses to viral infection. Besides IL-10, IL-12 and type I IFN, other cytokines and signaling molecules affect MV-mediated immunomodulation. Further analysis is needed to clarify the function of DCs that modulate MV-induced immunosuppression.

Acknowledgements

We are grateful to Dr. M. Takeda (National Institute of Infectious Diseases, Japan) for fruitful discussions. This work was supported in part by Grants-in-Aid from the Ministry of Education, Science, and Culture (Specified Project for 'Carcinogenic Spiral') and the Ministry of Health, Labor, and Welfare of Japan, and by the Program of Founding Research Centers for Emerging and Reemerging Infectious Diseases (Host factors determining tropism and pathogenicity of zoonoses in association with innate immune system) and Japan Society for the promotion of Science Fellows (21–1368).

References

- Asselin-Paturel C, Boonstra A, Dalod M, Durand I, Yessaad N, Dezutter-Dambuyant C, et al. Mouse type I IFN-producing cells are immature APCs with plasmacytoid morphology. *Nat Immunol* 2001;2:1144–50.
- Boonstra A, Asselin-Paturel C, Gilliet M, Crain C, Trinchieri G, Liu YJ, et al. Flexibility of mouse classical and plasmacytoid-derived dendritic cells in directing T helper type 1 and 2 cell development: dependency on antigen dose and differential toll-like receptor ligation. *J Exp Med* 2003;197:101–9.
- Coughlin MM, Bellini WJ, Rota PA. Contribution of dendritic cells to measles virus induced immunosuppression. *Rev Med Virol* 2013;23:126–38.
- de Swart RL, Ludlow M, de Witte L, Yanagi Y, van Amerongen G, McQuaid S, et al. Predominant infection of CD150+ lymphocytes and dendritic cells during measles virus infection of macaques. *PLoS Pathog* 2007;3:e178.
- de Witte L, Abt M, Schneider-Schaulies S, van Kooyk Y, Geijtenbeek TB. Measles virus targets DC-SIGN to enhance dendritic cell infection. *J Virol* 2006;80:3477–86.
- Delpout S, Noyce RS, Situ RW, Richardson CD. Host factors and measles virus replication. *Curr Opin Virol* 2012;2:773–83.
- Duhen T, Herschke F, Azocar O, Druelle J, Plumet S, Delprat C, et al. Cellular receptors, differentiation and endocytosis requirements are key factors for type I IFN

response by human epithelial, conventional and plasmacytoid dendritic infected cells by measles virus. *Virus Res* 2010;152:115–25.

- Edwards AD, Diebold SS, Slack EM, Tomizawa H, Hemmi H, Kaisho T, et al. Toll-like receptor expression in murine DC subsets: lack of TLR7 expression by CD8 alpha+ DC correlates with unresponsiveness to imidazoquinolines. *Eur J Immunol* 2003;33:827–33.
- Ferreira CS, Frenze M, Leonard VH, Welstead GG, Richardson CD, Cattaneo R. Measles virus infection of alveolar macrophages and dendritic cells precedes spread to lymphatic organs in transgenic mice expressing human signaling lymphocytic activation molecule (SLAM, CD150). *J Virol* 2010;84:3033–42.
- Gack MU, Shin YC, Joo CH, Urano T, Liang C, Sun L, et al. TRIM25 RING-finger E3 ubiquitin ligase is essential for RIG-I-mediated antiviral activity. *Nature* 2007;446:916–20.
- Gerlier D, Valentin H. Measles virus interaction with host cells and impact on innate immunity. *Curr Top Microbiol Immunol* 2009;329:163–91.
- Hahn B, Arbour N, Nanche D, Homann D, Manchester M, Oldstone MB. Measles virus infects and suppresses proliferation of T lymphocytes from transgenic mice bearing human signaling lymphocytic activation molecule. *J Virol* 2003;77:3505–15.
- Hahn B, Arbour N, Oldstone MB. Measles virus interacts with human SLAM receptor on dendritic cells to cause immunosuppression. *Virology* 2004;323:292–302.
- Hahn B, Cho JH, Oldstone MB. Measles virus–dendritic cell interaction via SLAM inhibits innate immunity: selective signaling through TLR4 but not other TLRs mediates suppression of IL-12 synthesis. *Virology* 2007;358:251–7.
- Hahn B, Trifilo MJ, Zuniga EI, Oldstone MB. Viruses evade the immune system through type I interferon-mediated STAT2-dependent, but STAT1-independent, signaling. *Immunity* 2005;22:247–57.
- Jarrossay D, Napolitani G, Colonna M, Sallusto F, Lanzavecchia A. Specialization and complementarity in microbial molecule recognition by human myeloid and plasmacytoid dendritic cells. *Eur J Immunol* 2001;31:3388–93.
- Kadowaki N, Ho S, Antonenko S, Malefyt RW, Kastelein RA, Bazan F, et al. Subsets of human dendritic cell precursors express different toll-like receptors and respond to different microbial antigens. *J Exp Med* 2001;194:863–9.
- Kato H, Takeuchi O, Mikamo-Satoh E, Hirai R, Kawai T, Matsushita K, et al. Length-dependent recognition of double-stranded ribonucleic acids by retinoic acid-inducible gene-1 and melanoma differentiation-associated gene 5. *J Exp Med* 2008;160:1–10, J205.
- Kawai T, Akira S. The roles of TLRs, RLRs and NLRs in pathogen recognition. *Int Immunol* 2009;21:317–37.
- Koga R, Ohno S, Ikegame S, Yanagi Y. Measles virus-induced immunosuppression in SLAM knock-in mice. *J Virol* 2010;84:5360–7.
- Kumagai Y, Takeuchi O, Kato H, Kumar H, Matsui K, Morii E, et al. Alveolar macrophages are the primary interferon-alpha producer in pulmonary infection with RNA viruses. *Immunity* 2007;27:240–52.
- Lazear HM, Lancaster A, Wilkins C, Suthar MS, Huang A, Vick SC, et al. IRF-3, IRF-5, and IRF-7 coordinately regulate the type I IFN response in myeloid dendritic cells downstream of MAVS signaling. *PLoS Pathog* 2013;9:e1003118.
- Lee HK, Lund JM, Ramanathan B, Mizushima N, Iwasaki A. Autophagy-dependent viral recognition by plasmacytoid dendritic cells. *Science* 2007;315:1398–401.

- Lemon K, de Vries RD, Mesman AW, McQuaid S, van Amerongen G, Yüksel S, et al. Early target cells of measles virus after aerosol infection of non-human primates. *PLoS Pathog* 2011;7:e1001263.
- Luber CA, Cox J, Lauterbach H, Fancke B, Selbach M, Tschopp J, et al. Quantitative proteomics reveals subset-specific viral recognition in dendritic cells. *Immunity* 2010;32:279–89.
- Mühlebach MD, Mateo M, Sinn PL, Prüfer S, Uhlig KM, Leonard VH, et al. Adherens junction protein nectin-4 is the epithelial receptor for measles virus. *Nature* 2011;480:530–3.
- Noyce RS, Bondre DG, Ha MN, Lin LT, Sisson G, Tsao MS, et al. Tumor cell marker PVRL4 (nectin 4) is an epithelial cell receptor for measles virus. *PLoS Pathog* 2011;7:e1002240.
- Ohno S, Ono N, Seki F, Takeda M, Kura S, Tsuzuki T, et al. Measles virus infection of SLAM (CD150) knockin mice reproduces tropism and immunosuppression in human infection. *J Virol* 2007;81:1650–9.
- Pfaller CK, Conzelmann KK. Measles virus V protein is a decoy substrate for IkappaB kinase alpha and prevents Toll-like receptor 7/9-mediated interferon induction. *J Virol* 2008;82:12365–73.
- Schlender J, Hornung V, Finke S, Günthner-Biller M, Marozin S, Brzózka K, et al. Inhibition of toll-like receptor 7- and 9-mediated alpha/beta interferon production in human plasmacytoid dendritic cells by respiratory syncytial virus and measles virus. *J Virol* 2005;79:5507–15.
- Sellin CI, Davoust N, Guillaume V, Baas D, Belin MF, Buckland R, et al. High pathogenicity of wild-type measles virus infection in CD150 (SLAM) transgenic mice. *J Virol* 2006;80:6420–9.
- Sellin CI, Jégou JF, Renneson J, Druelle J, Wild TF, Marie JC, et al. Interplay between virus-specific effector response and Foxp3 regulatory T cells in measles virus immunopathogenesis. *PLoS ONE* 2009;4:e4948.
- Shingai M, Inoue N, Okuno T, Okabe M, Akazawa T, Miyamoto Y, et al. Wild-type measles virus infection in human CD46/CD150-transgenic mice: CD11c-positive dendritic cells establish systemic viral infection. *J Immunol* 2005;175:3252–61.
- Takaki H, Honda K, Atarashi K, Kobayashi F, Ebihara T, Oshiumi H, et al. MAVS-dependent IRF3/7 bypass of interferon β -induction restricts the response to measles infection in CD150Tg mouse bone marrow-derived dendritic cells. *Mol Immunol* 2014;57:100–10.
- Takaki H, Takeda M, Tahara M, Shingai M, Oshiumi H, Matsumoto M, et al. The MyD88 pathway in plasmacytoid and CD4+ dendritic cells primarily triggers Type I IFN production against measles virus in a mouse infection model. *J Immunol* 2013;191:4740–7.
- Tatematsu M, Nishikawa F, Seya T, Matsumoto M. Toll-like receptor 3 recognizes incomplete stem structures in single-stranded viral RNA. *Nat Commun* 2013;4:1833.
- Tatsuo H, Ono N, Tanaka K, Yanagi YSLAM. (CDw150) is a cellular receptor for measles virus. *Nature* 2000;406:893–7.
- Vremec D, Pooley J, Hochrein H, Wu L, Shortman K. CD4 and CD8 expression by dendritic cell subtypes in mouse thymus and spleen. *J Immunol* 2000;164:2978–86.
- Wang Y, Swiecki M, Cella M, Alber G, Schreiber RD, Gilfillan S, et al. Timing and magnitude of type I interferon responses by distinct sensors impact CD8^T cell exhaustion and chronic viral infection. *Cell Host Microbe* 2012;11:631–42.
- Welstead GG, Iorio C, Draker R, Bayani J, Squire J, Vongpunsawad S, et al. Measles virus replication in lymphatic cells and organs of CD150 (SLAM) transgenic mice. *Proc Natl Acad Sci U S A* 2005;102:16415–20.
- Wies E, Wang MK, Maharaj NP, Chen K, Zhou S, Finberg RW, et al. Dephosphorylation of the RNA sensors RIG-I and MDA5 by the phosphatase PP1 is essential for innate immune signaling. *Immunity* 2013;38:437–49.
- Yamaguchi M, Kitagawa Y, Zhou M, Itoh M, Gotoh B. An anti-interferon activity shared by paramyxovirus C proteins: inhibition of toll-like receptor 7/9-dependent alpha interferon induction. *FEBS Lett* 2014;588:28–34.

The J6JFH1 Strain of Hepatitis C Virus Infects Human B-Cells with Low Replication Efficacy

Masato Nakai,^{1,2} Tsukasa Seya,¹ Misako Matsumoto,¹ Kunitada Shimotohno,³
Naoya Sakamoto,² and Hussein H. Aly^{1,*}

Abstract

Hepatitis C virus (HCV) infection is a serious health problem worldwide that can lead to hepatocellular carcinoma or end-stage liver disease. Current treatment with pegylated interferon, ribavirin, and NS3/4A protease inhibitor would lead to a good prognosis in a large population of patients, but there is still no effective vaccine for HCV. HCV robustly infects hepatocytes in the liver. However, extrahepatic manifestations such as mixed cryoglobulinemia, a systemic immune complex-mediated disorder characterized by B-cell proliferation, which may evolve into overt B-cell non-Hodgkin's lymphoma, have been demonstrated. HCV-RNA is often found to be associated with peripheral blood lymphocytes, suggesting a possible interaction with peripheral blood mononuclear cells (PBMCs), especially B-cells with HCV. B-cell HCV infection was a matter of debate for a long time, and the new advance in HCV *in vitro* infectious systems suggest that exosome can transmit HCV genome to support "infection." We aimed to clarify the susceptibility of primary B-cells to HCV infection, and to study its functional effect. In this article, we found that the recombinant HCV J6JFH1 strain could infect human B-cells isolated from the peripheral blood of normal volunteers by the detection of both HCV-negative-strand RNA by reverse transcription polymerase chain reaction, and NS5A protein. We also show the blocking of HCV replication by type I interferon after B-cell HCV infection. Although HCV replication in B-lymphocytes showed lower efficiency, in comparison with hepatocyte line (Huh7) cells, our results clearly demonstrate that human B-lymphocytes without other non-B-cells can actually be infected with HCV, and that this interaction leads to the induction of B-cells' innate immune response, and change the response of these cells to apoptosis.

Introduction

CHRONIC INFECTION BY HEPATITIS C VIRUS (HCV) is the major cause of liver cirrhosis and hepatocellular carcinoma. About 3.1% of the global population is infected with HCV (50). Historically, a combination therapy with pegylated interferon (IFN) and ribavirin was used for patients infected with genotype 1 HCV. NS3/4A protease inhibitors were recently developed in addition to pegylated IFN and ribavirin, and their combinations have been clinically tried for HCV treatment since then. Although >70% of patients with high viral loads of HCV genotype 1b have a sustained viral response by the therapy using simeprevir or telaprevir with pegylated IFN and ribavirin (17,22), the remaining patients fail to eliminate the virus, and drug resistance remains an issue that must be resolved. Recent development of direct-acting antiviral (DAA) drugs (such as daclatasvir, asuna-

previr, and sofosbuvir) are a promising therapeutic option beyond IFN in the treatment of HCV patients (6,32).

HCV is a single-stranded, positive-sense RNA virus in the Hepacivirus genus of the Flaviviridae family. Although HCV is known to infect hepatocytes in the liver and induce hepatitis *in vivo*, *in vitro* cultured primary hepatocytes barely support the HCV life cycle: only hepatoma Huh7 cells and its subclones can efficiently maintain the HCV life cycle of a very limited number of HCV strains *in vitro* (53).

Chronic hepatitis patients with HCV sometimes show other extrahepatic complications such as lymphoproliferative diseases (LPD), including cryoglobulinemia and B-cell malignant lymphoma, autoimmune diseases, and dermatitis (1,12,15,16). Epidemiological analysis shows that chronic HCV patients have higher rates of LPDs than non-HCV-infected populations (36,48,52). Several reports suggested that some lymphotropic HCV strains effectively infected human

Departments of ¹Microbiology and Immunology, and ²Gastroenterology, Hokkaido University Graduate School of Medicine, Kita-ku, Japan.

³Research Center for Hepatitis and Immunology, National Center for Global Health and Medicine, Ichikawa, Japan.

*Present affiliation: Department of Virology II, National Institute of Infectious Diseases, Toyama, Tokyo, Japan.

lymphocytes (20,47), leading to the above-mentioned abnormalities. Infection of lymphocytes with HCV has been a matter of debate for a long time. More than one decade ago, several reports described the existence of HCV-RNA in peripheral blood mononucleated cells (PBMCs) (30,40). The detection rate of HCV-RNA in PBMCs was increased if patients were infected with human immunodeficiency virus (HIV) together with HCV (44). This phenomenon indicated that immune-suppressive circumstances and/or HIV antigen might enhance the replication activity of HCV in lymphoid cells (44). Moreover, it was reported that continuous release of HCV by PBMCs was detected in HCV-infected patients, especially in HIV co-infected patients (7). In addition to HCV-HIV co-infected patients, a low level of HCV replication could be detected in peripheral lymphoid cells from HCV mono-infected patients after antiviral treatment (34,45). Moreover, it was reported that HCV persisting at low levels long after therapy-induced resolution of chronic hepatitis C remained infectious (34). This continuous viral presence could present a risk of infection reactivation.

It has been reported that HCV replication was detected in various kinds of lymphoid cells. Many reports describing the existence of HCV in B-lymphocytes and B-cell lymphoma have been published (21,25,51). Among B-lymphocytes, CD27+ memory B-lymphocytes were more resistant to apoptosis than CD27- B-lymphocytes. CD27+ B-lymphocytes were reported as a candidate subset of the HCV reservoir in chronic hepatitis C (CH-C) (38). On the other hand, others claimed that distinguishing RNA association from true HCV replication was problematic, together with multiple artifacts complicated detection and quantitation of the replicative intermediate minus strand RNA (29,31), and also the failure of retroviral (37) and lentiviral (8) pseudoparticles bearing HCV envelope glycoproteins (HCVpp) to infect primary B-cells or B-cell lines. This led to continuous debate about HCV infection into B-lymphocytes, and the riddle remained unsolved.

Using the recent progress in HCV infection systems, we intended to clarify this debate and analyze HCV infection in human lymphocytes and its functional results. Here, albeit in a lower efficiency compared to HCV infection into Huh7 cells, we report that two different strains of recombinant HCV viruses could infect primary human lymphocytes not only by the detection of HCV-RNA positive and negative strands proliferation, but also NS5A protein detection, and the detection of the activity of luciferase reporter encoded by the recombinant HCV-genome. Blocking of HCV entry using anti-CD81 antibody (Ab), and replication by IFN- α or NS3/4A protease inhibitors successfully suppressed HCV infection. We also found that HCV infection into B-lymphocytes led to the initiation of host response including apoptosis resistance.

Materials and Methods

Cells and reagents

Huh7.5.1 cells were kindly provided by Dr. Francis V Chisari (The Scripps Research Institute, La Jolla, CA). Cells were cultured in high-glucose Dulbecco's modified Eagle's medium (DMEM; Gibco/Invitrogen, Tokyo, Japan) supplemented with 2 mM L-Glutamine, 100 U of penicillin/mL, 100 μ g of streptomycin/mL, 1 \times MEM non-essential amino acid (Gibco/Invitrogen), and 10% fetal bovine serum (FBS).

Human peripheral blood mononuclear cells (PBMCs) were obtained from healthy volunteers by density gradient centrifugation using Ficoll Paque plus (GE-Healthcare, Waukesha, WI). CD19+ blood cells (representative of human primary B-cells) and CD19- cells (non-B-cells) were separated by MACS CD19 Beads (Milteny Biotec, Bergisch Gladbach, Germany). Purity of CD19+ B-cells was >95% after two-cycle separation. The cells were cultured in RPMI1640 (Gibco/Invitrogen) supplemented with 100 U of penicillin/mL, 100 μ g of streptomycin/mL, and 10% FBS.

The following reagents were obtained as indicated: anti-CD81 Ab (BD Pharmingen, Franklin Lakes, NJ); PE anti-CD80 Ab, APC anti-CD86 Ab, and PE-labeled anti-CD19 Ab (eBioscience, San Diego, CA); recombinant IFN- α (Peprotech, Oak Park, CA); BILN2601 (Behringer, Willich, Germany); and Viaprobe 7AAD (BD Bioscience) and Annexin-V-Fluos (Roche, Mannheim, Germany).

Virus propagation

pJ6-N2X-JFH1 was kindly provided from Dr. Takaji Wakita (National Institute of Infectious Diseases, Tokyo) (2). pJc1-GLuc2A was gifted from Dr. Brett D. Lindenbach (Yale University, New Haven) (41). *In vitro* RNA transcription, gene transfection into Huh7.5.1 cells, and preparation of J6JFH1 and Jc1/GLuc2A viruses were performed as previously reported (53). Briefly, the HCV cDNA in plasmids were digested by XbaI and transcribed by T7 Megascript Kit (Invitrogen, Carlsbad, CA). RNA transfection into Huh7.5.1 was performed by electroporation using Gene Pulser II (Bio-Rad, Berkeley, CA) at 260 V and 950 Cap. Culture supernatant were collected on days 3, 5, 7, and 9 of postelectroporation, and concentrated with an Amicon Ultra-15 Centrifugal Filter unit (Millipore, Billerica, MA). The titer of HCVcc was checked by the immunofluorescence method using NS5A antibody when Huh7.5.1 was reinfected with these HCVcc.

Virus infection

Primary B-cells and non-B-cells were cultured with the J6JFH1 HCV strain at a multiplicity of infection (MOI) = 1–3 for 3 h, and cells were harvested after four extensive washes in culture medium. On days 1–6, cells were collected, washed with 0.25% trypsin-EDTA/saline, and incubated with 0.25% trypsin-EDTA for 5 min at 37°C. Then, suspended cells were collected as a source of total RNA. In some experiments, B-cells were infected with the Jc1/GLuc2A strain at MOI = 5 for 3 h. Cells were washed five times in 1 \times phosphate buffered saline (PBS), and cultured until day 6 for determination of viral replication as GLuc activity with BioLux Gaussia luciferase assay kits (41).

RNA purification, RT-PCR, and quantitative PCR

Total RNA was extracted by using Trizol Reagent (Invitrogen) according to the manufacturer's instructions. Using 100–400 ng of total RNA as a template, we performed RT-PCR and real-time RT-PCR as previously described (3,4). Primer sets are shown in Supplementary Table S1 and Table S2 (Supplementary Data are available online at www.liebertpub.com/vim).

Real-time PCR was used for quantification of positive-strand and negative-strand HCV RNA. Total Trizol-extracted

RNA was analyzed by RT-PCR with a modification of the previously described strand-specific rTth RT-PCR method (10,13). RT primers for complementary DNA synthesis of positive and negative strand HCV RNA are shown in Supplementary Table S1. Positive-strand and negative-strand HCV PCR amplifications were performed using Power SYBR Green PCR Master Mix (Applied Biosystems, Warrington, UK) with 200 nM of paired primers (Supplementary Table S1). The PCR conditions were 95°C for 10 min, followed by 40 cycles at 95°C for 15 sec and 60°C for 1 min.

Virus production and releasing assay

Primary human B-cells were infected with J6JFH1 at MOI=1. Six days postinfection, the supernatant was collected ("releasing samples"), cells were repeatedly frozen and thawed, and the supernatant was collected ("assembly samples"). Viral titers of "releasing samples" and "assembly samples" were determined with Huh7.5.1 cells using J6JFH1 virus (MOI=0.001 and 0.01) as control. Total RNA was recovered from the cells on days 2, 4, and 6, and determined with HCV-RNA to check reinfectivity.

Indirect immunofluorescence

Indirect immunofluorescence (IF) expression of HCV proteins was detected in the infected cells using rabbit IgG anti-NS5A antibody (Cl-1) (3). Goat anti-rabbit Alexa 594 (Invitrogen) was used as secondary Ab. Fluorescence detection was performed on the Zeiss LSM 510 Meta confocal microscope (Zeiss, Jena, Germany) (13).

Luciferase assay

Primary B-cells were infected with Jc1/Gluc2A by using concentrated Medium or Mock Medium (PBS-electroporated Huh7.5.1 medium). Media were collected on days 0, 2, 4, and 6 postinfection, cleared by centrifugation (16,000 *g* for 5 min), and mixed with 0.25 volume of *Renilla* 5 lysis buffer (Promega, Madison, WI) to kill HCV infectivity. GLuc activity was measured on a Berthold Centro LB 960 luminescent plate reader (Berthold Technologies, Bad Wildbad, Germany) with each 20 μ L sample injected with 50 μ L BiLux Gaussia Luciferase Assay reagent (New England Biolabs, Ipswich, MA), integrated over 1 sec.

Cell survival assay

Apoptosis assay: Primary B cells were infected with J6JFH1 virus. Cells were collected 48 h after infection, stained by 7AAD Cell Viability assay kit and Annexin V, and analyzed by FACS Calibur (BD) (13).

ATP assay

Primary B-cells were infected with J6JFH1 virus or Mock concentrated medium. Cells were resuspended and cultured at Lumine plate (Berthold Technologies) postinfection. ATP activities were determined 72 h later using CellTiter-Glo[®] Luminescent Cell Viability Assay (Promega) according to the manufacturer's protocol.

miRNA detection

Total RNA was extracted by using Qiazol Reagent (Invitrogen). These RNA was purified and reverse transcribed

to cDNA by using the miScript II RT Kit. Synthesized cDNA was used to determine the expression levels of miR-122 (24). Total miRNA was prepared by using Qiazol and miScript II RT kit (Invitrogen), and miR-122 expression was determined by using miScript SYBR Green PCR Kit and miScript Primer Assay (Invitrogen) according to the manufacturer's protocol. U6 small nuclear RNA was used as an internal control.

Results

J6JFH1 infects and replicates in primary B-cells

To address HCV infectivity into primary B-cells, PBMC were isolated from the blood of healthy volunteers and were sorted into CD19+ cells (primary B-lymphocytes) and CD19- cells (non-B-cells). Their purities were >95%. These cells were then incubated with the J6JFH1 HCV. Total RNA was collected on days 2, 4, and 6. The Huh7.5.1 strain was used as positive control. Both Huh7.5.1 and primary B-cells, but not non-B-cells, showed an increase in intracellular HCV-RNA titer, albeit primary B-cells showed lower efficiency than Huh7.5.1 (Fig. 1A). We adjusted the HCV-RNA values using GAPDH as an internal control (Fig. 1B). To confirm J6JFH1 replication in primary B-cells using IF, we also measured the expression of HCV-NS5A, which is a nonstructural protein produced only by the virus secondary to replication. Although the expression was far lower than Huh7.5.1 cells, we managed to detect the NS5A expression in J6JFH1 infected primary B-cells (Fig. 1C).

We examined what kinds of HCV-entry receptors human primary B-cells expressed in our setting. Human CD81, SRB1, and NPC1L1 were expressed, but not the tight junction proteins claudin1 and occludin in mRNA levels (Supplementary Fig. S1). We could not detect miR122 in primary B-cells (Supplementary Fig. S2), expression of which makes the cells permissive to HCV (24). Human CD81 is a primary entry receptor for HCV in hepatocytes (42). Blocking human CD81 by its specific Ab resulted in blockage of HCV infection into primary B-cells, as shown by the suppression of HCV-RNA titer (Fig. 2), suggesting that HCVcc particles enter B-cells also using CD81 receptor. HCV-RNA titer was not suppressed by non-specific Ab (data not shown).

We then examined the effect of the different drugs used to suppress HCV replication (recombinant human IFN, and HCV protease inhibitor, BILN2601). Inhibition of HCV-RNA replication was observed when B-cells were treated with rhIFN- α or BILN2601 (Fig. 2) after infection. BILN2601 showed efficient inhibitory effect on replication of HCV RNA in Huh7.5.1 cells (Supplementary Fig. S3). As control studies, we confirmed that the production of HCV RNA was reduced in Huh7.5.1 cells by CD81 Ab, IFN- α , or BLIN2601 (Supplementary Fig. S4). In both Huh 7.5.1 and B-cells, BLIN2601 most effectively block HCV replication. These data reinforce that HCV is actually replicating in primary B-cells, and that activation of innate immunity by IFN treatment or blocking the NS3/4A protease function is a critical factor in blocking HCV replication in primary B-cells. These data suggest that our system can be used for screening the function of different inhibitors on HCV replication in B-cells.

HCV negative-strand RNA detected in human B-cells

To confirm HCV replication in primary B-cells further, we tested for an increase of negative-strand HCV-RNA after

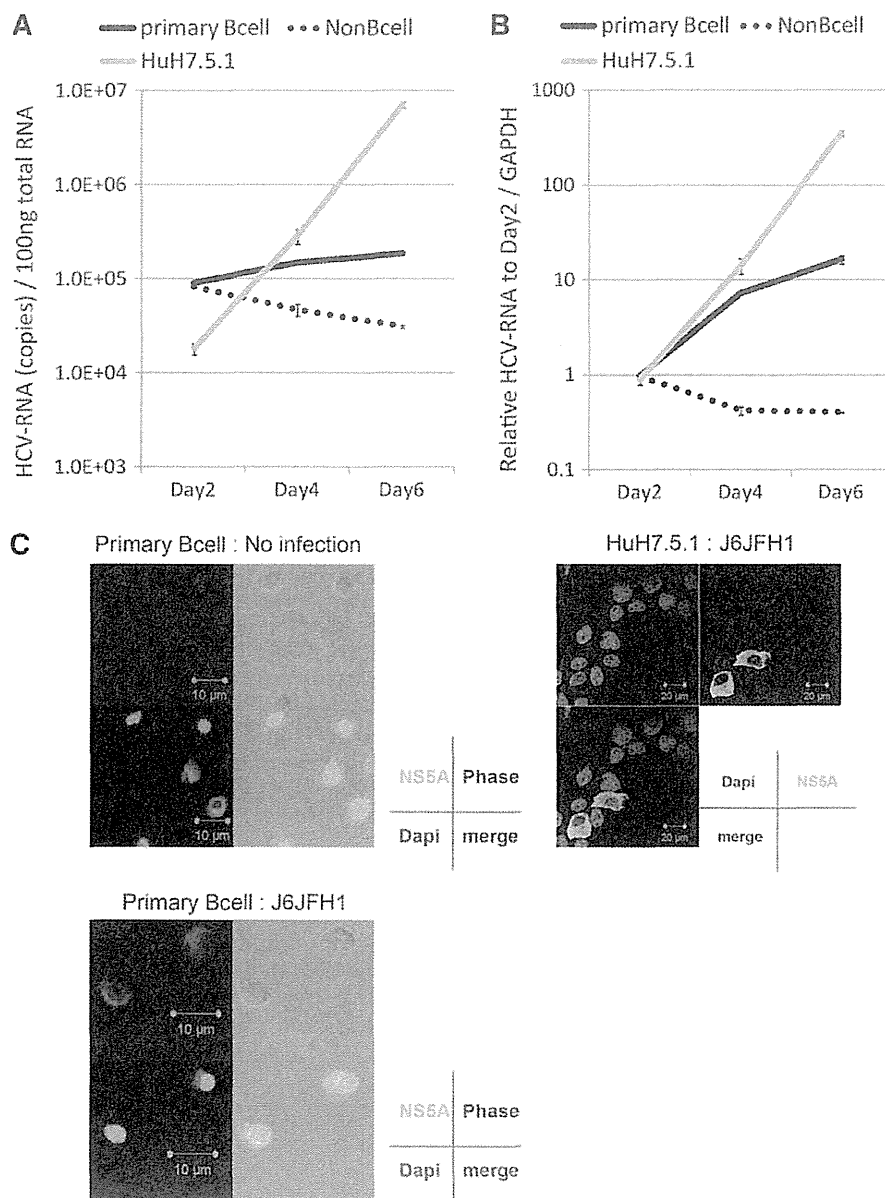


FIG. 1. J6JFH1 infects human peripheral blood B-cells. Human B-cells (CD19⁺ cells) and non-B-cells (CD19⁻ cells) were separated by MACS as described in Materials and Methods. Primary B-cells, non-B-cells, and Huh7.5.1 cells were infected with J6JFH1 at MOI=1 for 3 h. After infection, cells were washed twice with culture medium and continued culture. On days 2, 4, and 6, total RNA was collected and HCV-derived RNA was determined by reverse transcription polymerase chain reaction (RT-PCR). GAPDH was used as internal control. (A) HCV-RNA not adjusted by GAPDH. (B) HCV-RNA adjusted by GAPDH. (C) Immunofluorescence analysis of J6JFH1-infected human B-cells and Huh7.5.1 cells. Six days postinfection. Red, NS5A; blue: Dapi; phase: phase-shift microscope.

infection, since the negative-strand RNA is not yielded if HCV particles or RNA just adhere to the cell surface of human primary B-cells without internalization (9,14,19,35, 42,43). We measured the synthesis of plus-strand and minus-strand HCV-RNA separately using strand-specific RT primers and rTth polymerase as previously described (4). The titer increase of minus-strand HCV-RNA indicates HCV-RNA replication. As shown in Figure 3, both minus-

and plus-strand HCV-RNA increased time dependently in primary B-cells, and both types of RNA concomitantly decreased in non-B-cells (Fig. 3A and B). Plus- and minus-strand RNA were exponentially increased in Huh7.5.1 cells infected with J6JFH1 (Fig. 3C). These results indicated that primary human B-cells supported J6JFH1 infection and replication, although viral replication levels in B-cells were modest compared with those in Huh7.5.1 cells. These results

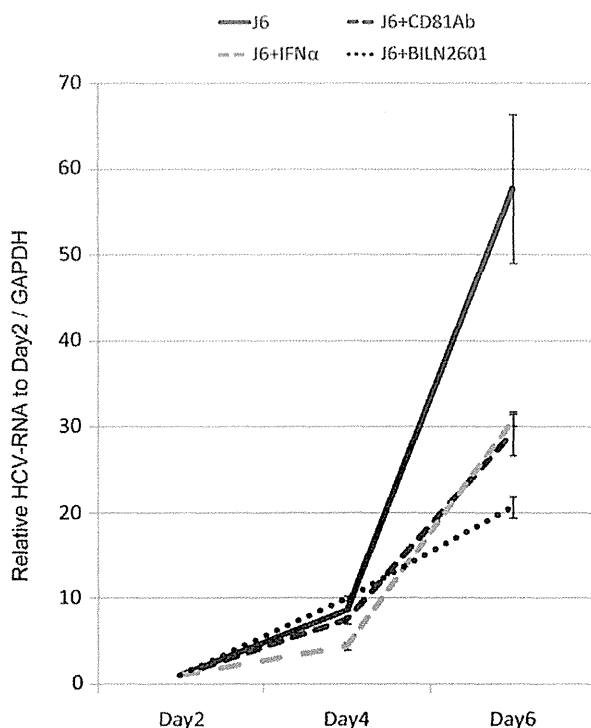


FIG. 2. J6JFH1 B-cell infection is blocked by anti-CD81 Ab, IFN- α , or an NS3/4A inhibitor. Anti-CD81 neutralizing Ab (20 μ g/mL) was added to the B-cell culture 1 h before infection. Otherwise, recombinant IFN- α rhIFN- α , 200 IU/mL or BLIN2601 (250 nM, which is IC75; see Supplementary Fig. S3) was added 1 h after infection. On days 2, 4, and 6, total RNA was extracted, and HCV-RNA was determined by RT-PCR. The values were adjusted by GAPDH.

may reflect the fact that the NS5A protein is difficult to detect in infected B-cells using IF assay.

B-cells can be infected with different HCV strains

We next used the Jc1/GLuc2A strain to investigate whether different HCV strains infect primary B-cells. Primary B-cells, non-B-cells (data not shown), and Huh7.5.1 cells were infected with the Jc1/GLuc2A strain. After five washes, supernatant was collected (day 0 samples). On days 2, 4, and 6, medium was collected. Luciferase activity was determined for all samples by luminescence (GLuc). GLuc activity and detection of RNA increased exponentially in Huh7.5.1 cells infected with the Jc1/GLuc2A strain (Fig. 4A). GLuc activity on day 4 to day 6 increased more in primary B-cells than in non-B-cells (Fig. 4B). These results suggest that HCV replication is substantial, but low in the HCV line Jc1/GLuc2A.

B-cells neither produce nor release detectable level of HCV infectious particles

We collected supernatants of J6JFH1-infected primary human B-cells to measure productive infection in B-cells. The supernatant was then added to culture of Huh7.5.1 cells, and we compared infection with control Huh7.5.1 cells, whose

cells were infected with a low MOI (0.01 and 0.001) of J6JFH1 collected from media of the infected Huh7.5.1 cells. HCV-RNA titer in the Huh7.5.1 titrating cells was decreased over time after co-culture with B-cell supernatants obtained from either "releasing samples" "assembly samples." In contrast, HCV-RNA titers were slightly increased over time in the Huh7.5.1 titrating cells that had been infected with medium collected from low MOI-J6JFH1-infected Huh7.5.1 cells (Fig. 5). These results indicated that primary human B-cells were infected with J6JFH1 but failed to assemble or produce particles into the supernatant.

Host response to HCV infection into primary B-cells

Next, we determined whether B-cell activation was induced in HCV-infected B-cells that survived under HCV infection. We measured induction of CD80 and CD86 as B-cell activation markers. After 2–3 days of infection, the CD80/86 levels on B-cells treated with J6JFH1 were compared with those treated with medium from mock-infected cells (concentrated Huh7.5.1 medium) by FACS analysis (Fig. 6A). We found that CD80/86 were upregulated in infected cells compared to mock-infected cells.

Since B-cell lymphoma is a known complication of chronic HCV infection (20,36) and acquiring apoptotic resistance is essential for the development of cancer (21,51,38), we measured the ability of B-cells to escape apoptosis after HCV infection. B-cell apoptosis spontaneously occurs during culture at 37°C. The percent of apoptosis of primary B-cells was decreased in FACS analysis using 7AAD viaprobe + annexinV (Fig. 6B) and ATP assays postinfection (Fig. 6C). These results suggest that primary B-cells are protected from apoptosis by infection with HCVcc. It has been reported that B-cells were vulnerable to apoptotic cell death at various stages of peripheral differentiation and during signal responses (18). Thus, the results infer that HCV stimulation interferes with B-cell apoptotic signal in human B-cells.

Discussion

We show evidence suggesting that human peripheral B-cells can be infected with HCV strains. Establishment of J6JFH1 infection was evaluated by minus-strand PCR amplification, production of core and NS5A proteins, and protection from apoptosis. An increase in HCV RNA in B-cells was inhibited by an exogenously added antibody against CD81 that blocked HCV receptor function. Furthermore, blocking HCV replication in B-cells by type I IFN and NS3/4A protease inhibitor confirmed the presence of HCV infection/replication in human B-cells. The results were corroborated with another HCV strain, Jc1/GLuc2A. Although we failed to establish an EBV-transformed B-cell line to reproduce HCV infection of B-cells, peripheral blood B-cells were infected with J6JFH1 in 12 independent experiments.

One of the well-known complications of chronic HCV infection is LPD, including cryoglobulinemia and B-cell malignant lymphoma, indicating the involvement of B-cells in the course of the disease (1,12,15,16). However, many reports describing the existence of the HCV genome in B-cells and lymphomas (21,25,51) and HCV replication in B-cells have been controversial due to multiple artifacts complicated in detection and quantitation of the replicative

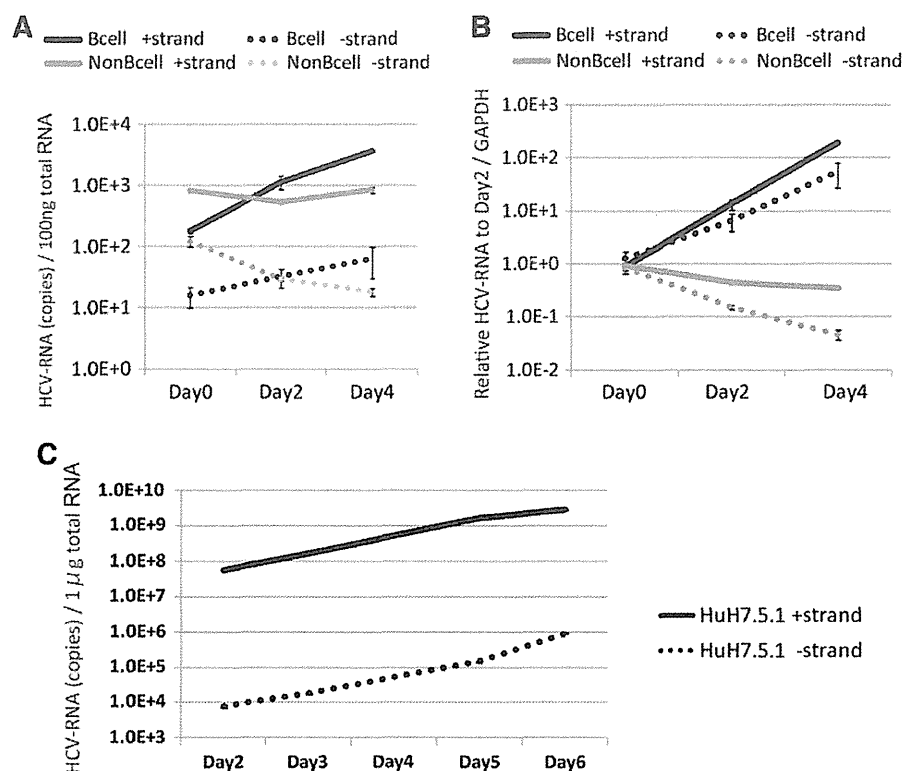


FIG. 3. HCV negative strand RNA is detected in human B-cells. By using rTth methods, HCV strand-specific RNA was determined in J6JFH1-infected human B-cells. (A) Not only plus strand HCV-RNA but also minus strand HCV-RNA were increased in a time-dependent manner in human B-cells. (B) When HCV-RNA was adjusted by GAPDH that was used as an internal control, HCV-RNAs in B-cells were substantially increased compared with those in non-B-cells. (C) Plus and minus strand HCV-RNAs were efficiently amplified in J6JFH1-infected Huh 7.5.1 cells. The level of HCV-RNA exponentially increased in this hepatocyte line.

intermediate minus strand RNA (29,31). This has led to a continuous debate about HCV infection in B-lymphocytes.

HCV entry into B-cells has also been previously reported to be absent because retroviral (37) and lentiviral (8) pseudoparticles bearing HCV envelope glycoproteins (HCVpp) did not infect primary B-cells or B-cell lines. In our study, while we succeeded in infecting Huh7.5.1 cells efficiently with retroviral pseudoparticles for expressing both HCV E1/E2 and the control VSV-G, we failed to establish the same infection in B-cells, suggesting that the block of pseudoparticle entry into B-cells is not related to HCV glycoproteins alone.

Total PBMCs reportedly facilitate HCV attachment but not internalization (42), so HCV infection of B-cells is abrogated in total PBMCs (35). The cause of HCV absorption is unclear, but incomplete sets of HCV receptors in non-B PBMC cells permit attachment of HCV without internalization. B-cells possess CD81, SRBI, LDL-R, and NPC1L1. Because B-cells are not adherent cells, they do not express claudin 1 and occludin, which forms a receptor complex for HCV (9,14,19,43). Claudin 1 and occludin are components of tight junctions and serve as HCV receptors in human hepatocytes. In infection studies using cells expressing these proteins, however, claudin 1 and occludin only upgrade infection efficacy and are dispensable to infection (5), al-

though CD81 is essential for establishment of infection (42). Lack of claudin 1 and occludin or miR122 might be a cause of the low HCV infection efficiency observed in human B-cells. Function blocking of CD81 by its specific antibody suppressed HCV infection in primary B-lymphocytes, which imply that HCV entry into primary B-lymphocyte is dependent on the direct interaction phenomenon between HCV virus particles and CD81 receptor and is not mediated by other nonspecific (CD81 independent) pathways such as exosomal transfer of HCV from Huh7 cells to nonhepatic cells, such as dendritic cells (46).

Previous report using *in vitro* prepared recombinant HCV JFH1 particles (HCVcc) failed to establish HCV infection in B-lymphocyte cell lines (39). While HCV is known to infect human hepatocytes *in vivo* leading to chronic viral hepatitis, in the *in vitro* conditions, only the combination between Huh7 cells and its derived clones supported robust replication and infection with only JFH1 or its derived chimeras (5). Neither hepatocyte cell lines including primary hepatocytes nor other HCV strains could reproduce HCV infection efficiently *in vitro* (5). These data suggest that the clonal selection of HCV quasiespecies by hepatoma Huh7 cells is essential for this robust infection *in vitro*. The situation would be similar to the JFH1 story in B-cell HCV infection.

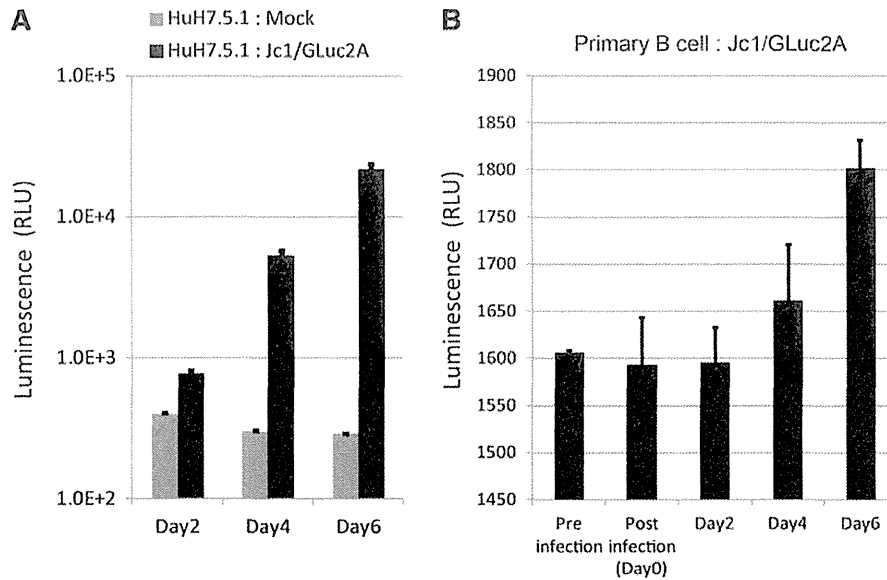


FIG. 4. Jc1/GLuc2A strain infects human B-cells with an increase of Gluc activity. Human B-cells and Huh7.5.1 cells were infected with the Jc1/GLuc2A strain that contains secretory luciferase derived from *Gaussia* (GLuc) at MOI=5. Huh7.5.1 cells were used as control. GLuc activity was increased as time cultured. The GLuc activity was saturated in Huh7.5.1 (A). On the other hand, GLuc activity was increased from day 4 in human B-cells (B).

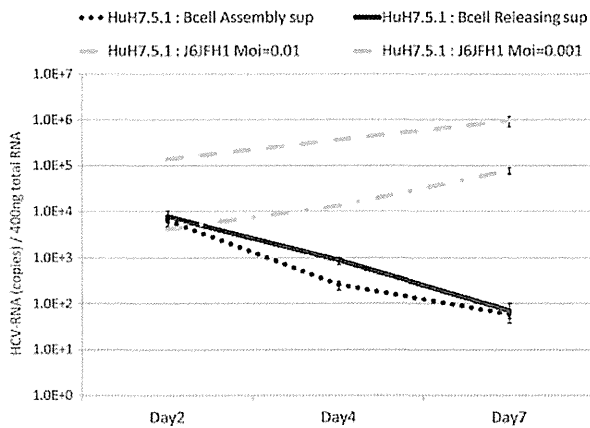


FIG. 5. B-cells infected with J6JFH1 fail to produce virus particles. Human B-cells were infected with J6JFH1 for 3 h, washed twice with phosphate buffered saline (PBS), and cultured. Six days after infection, the supernatant was collected (“releasing samples”). Cells were periodically frozen and thawed five times, and the supernatant was collected (“assembly samples”). For evaluation of the infectious virions, Huh7.5.1 cells were treated with these “releasing samples” or “assembly samples.” Similarly, Huh7.5.1 cells were treated with J6JFH1 at low MOI (MOI=0.01 and 0.001) in parallel. After the treatment, cells were washed and cultured. On days 2, 4, and 7, cells were harvested to collect HCV-RNA. Total RNA was extracted from each samples, and HCV-RNA was determined by RT-PCR methods.

B-cell apoptosis spontaneously occurs during culture at 37°C. We found that B-cell apoptosis was blocked by J6JFH1 infection, as reported previously using Raji cells (11). B-cell apoptosis usually occurs secondary to viral infection, but HCV is particular since apoptotic signaling interferes with infection, leading to protection from cell death. However, B-cell survival was not due to primary infection, because the percent of cells circumventing apoptosis was usually higher than cells infected with HCV. We could not define the pathways that participated in apoptosis regulation by HCV, although a previous report (11) suggested that E2-CD81 engagement was related to B-lymphocyte disorders and weak neutralizing antibody response in HCV patients. Since B-cell lymphoma is a known complication of chronic HCV infection (27), the inability of infected cells to undergo apoptosis can be associated with the development of cancer (28,33,49). In this context, B-cell lymphoma often occurs in mice with Cre-initiated HCV transgenes (26). It is notable that anti-apoptotic effect of HCV core gene was reported in genotype 3a in Huh7 cells (23) and, here, genotype 2a in B-cells. In another report (51), HCV strains established from B-cell lymphoma persistently infected with HCV were genotype 2b. B-cell HCV infection might not be linked to some specific genotypes of HCV.

We believe that our report shows that human primary B-cells can be infected *in vitro* with HCV, and that this infection is dependent on HCV particles binding with its receptor CD81 and is not nonspecific entry (e.g., exosomal mediated). We also show that this infection could be blocked with antibodies interfering with this binding, or with drugs that suppress HCV replication. Although no virion was generated from B-cells in HCV infection, it is still likely that B-cells serve as a temporal reservoir of HCV in the blood circulation. If B-cells permit HCV infection, RNA sensors